Atmos. Meas. Tech. Discuss., 7, 10159–10178, 2014
www.atmos-meas-tech-discuss.net/7/10159/2014/
doi:10.5194/amtd-7-10159-2014

Atmospheric Measurement Techniques
Discussions
Open Access

Micro-physical properties of carbonaceous aerosol particles generated by laser ablation of a graphite target

T. Ajtai[1], N. Utry[2], M. Pintér[2], Cs. Tápai[2], G. Kecskeméti[2], T. Smausz[1], B. Hopp[2], Z. Bozóki[1,2], and G. Szabó[2]

[1]Hungarian Academy of Sciences – University of Szeged (MTA-SZTE) Research Group on Photoacoustic Spectroscopy, 6720 Szeged Dóm tér 9, Hungary
[2]University of Szeged, Department of Optics and Quantum Electronics,
6720 Szeged Dóm tér 9, Hungary

Received: 12 June 2014 – Accepted: 9 September 2014 – Published: 30 September 2014

Correspondence to: T. Ajtai (ajtai@titan.physx.u-szeged.hu)

Published by Copernicus Publications on behalf of the European Geosciences Union.

Title Page
Abstract | Introduction
Conclusions | References
Tables | Figures
◀| |▶
◀ ▶
Back | Close
Full Screen / Esc
Printer-friendly Version
Interactive Discussion

Abstract

In this work the authors propose laser ablation as a highly versatile tool for carbonaceous aerosol generation. The generated carbonaceous particles can be used as a model aerosol for atmospheric black carbon. Various microphysical properties including mass concentration, size distribution and morphology of aerosol particles generated by laser ablation of a high purity graphite sample were investigated in detail. These measurements proved that the proposed method can be used to generate both primary particles and fractal aggregates with a high yield. As a further advantage of the method the size distribution of the generated aerosol can cover a wide range, and can be tuned accurately with laser fluence, the ambient composition or with the volumetric flow rate of the carrier gas.

1 Introduction

Combustion generated carbon particles – soot – have been in the focus of scientific interest, primarily because of their influence on climate as well as their adverse effects on human health (IPCC, 2007; Pope and Dockery, 1999). Moreover, according to the latest scientific assessment, atmospheric soot, which is the by-product of incomplete combustion of both fossil and biomass fuel as well as biomass burning, is the second most important anthropogenic emission. Only CO_2 has larger climatic impact. (Bond et al., 2013). Atmospheric soot is a mixture of most refractory particles having strong but featureless optical absorption properties called elemental carbon (EC) or black carbon (BC) and organic carbon (OC) that can have a wide range of thermal and optical absorption characteristics. Nevertheless, since atmospheric soot originates mainly from anthropogenic sources, its real-time and selective identification is also of crucial importance in terms of legal regulations (Kirschetter et al., 2005; Hand et al., 2005). The identification and characterisation of atmospheric soot is generally based on the measurement of its specific properties i.e. absorption and scattering or size and morphology as well as its composition and refractivity. Although, many instruments have been developed and optimized to measure these quantities, one of the major obstacles to reduce uncertainties associated with the measured data is the lack of a soot standard reference material which is able to model the specific properties of the atmospheric soot that is actually measured (Baumgarden et al., 2012). However, the parameters generally used to characterise atmospheric soot are very complex having great variety and depend not only on the initial burning conditions or the type of fuel but also on many environmental factors. Therefore, it is highly advantageous if the applied generation method can provide not only a model soot with a specific and complex set of parameters but can also modify all relevant properties independently from each other preferably in the entire climate and health relevant domains. The standard techniques based on specially designed gas burners and graphite electrode spark dischargers only partially fulfill the above mentioned requirements (Schnaiter et al., 2006, 2003), so introducing alternative methods for soot production is a relevant and actual scientific goal.

In this work, we propose a novel carbonaceous particle generation method based on laser ablation of a graphite target. We present the characteristic microphysical features of particles generated by our proposed method such as mass concentration, size distribution and morphology as a function of generation parameters including most importantly the fluence of the ablation laser as well as the flow rate and the composition of the carrier gas.

2 Experimental

The generation and characterisation of the carbonaceous aerosol particles were carried out in the following experimental arrangement (Fig. 1). KrF excimer laser (LLG TWINAMP) beam was focused by a fused silica lens onto the surface of the target material. The operational wavelength and the pulse duration (full width at half maximum) were 248 nm and 18 ns, respectively. The applied laser was operated at a 1 Hz repetition rate. The laser energy on the surface of the ablated sample was determined as follows. A quartz plate was installed into the laser beam, which served as an energy coupler reflecting 4 % of the laser energy onto the surface of an energy meter (Laser Probe Inc., Rm-3700). This value, when divided by the irradiated sample area (which was measured to be 2.5 mm^2) gives the laser fluence on the sample. The fluence was varied from 0.5–2.9 $J\,cm^{-2}$ during the reported measurements. The target material for aerosol generation was a high purity graphite disc (Goodfellow, purity > 99.95 %) with a diameter and thickness of 3 cm and 5 cm, respectively. The sample was placed and irradiated in an ablation chamber (Fig. 1), which was a modified version of a PLD (Pulsed Laser Deposition) chamber described in detail earlier (Ajtai et al., 2010; Hopp et al., 2011). The cylindrically shaped ablation chamber was made of stainless steel with an inner diameter and length of 3 and 10 cm, respectively. The focused laser beam was directed into the chamber through a fused silica window at an angle of 45° with respect to the surface of the irradiated sample. In order to minimize the loss of the generated particles, the purging gas inlet and the outlet were milled onto the opposite sides of the ablation chamber ensuring a straight gas flow path through the chamber. This was the most important modification of the chamber, as in a typical PLD experiment the generated particles do not leave the chamber, so the gas flow direction is irrelevant. To improve the stability of the yield of the ejected particles the target was placed onto a rotating sample holder, and the angular speed of rotation was matched to the repetition rate of the laser and the dimension of the irradiated spot in order to ensure uniform sample etching, i.e. quasi-homogeneous ablated target surface structure and consequently uniform material ejection over a long period of time. This way stable particle production could be realised for several hours. High purity nitrogen or synthetic air having 5.0 certified purity, as well as their mixtures was used as purging gas. The flow rate of purging gas was set and controlled by mass flow controllers (MFC, Tylan 2900FC). The generated carbonaceous particles were carried by the purging gas into a dilution chamber from which the measuring instruments sucked the aerosol-laden sample streams. All the reported experiments were performed at room temperature and atmospheric pressure, with the latter ensured by an exhaust pipe attached to the dilution chamber (Fig. 1).

The number concentration and size distribution of the generated particles were measured in the size range of 10 to 1100 nm with a Scanning Mobility Particle Sizer (SMPS, GRIMM system Aerosol Technik, Germany, type SMPS) in two subsequent steps. First, the sampled aerosol stream was lead into a Classifier "Vienna" Type Long Differential Mobility Analyser (LDMA, Model #5.500). The LDMA separates particles based on their mobility by balancing their drag and electrical force on the equally charged aerosol stream. Then the sized particles are sent to the Condensation Particle Counter (CPC Model #5.400) in which the size segregated particles are counted. In order to minimize the occurrence of the so called shielding artefact, in which case two or more particles arrive in the detection chamber simultaneously, coincide correction of the measured data was performed. The sheath and aerosol flow rate were set to 3.0 and 0.3 $\mathrm{L\,min^{-1}}$, respectively.

The mass concentration of the generated aerosol stream was measured by a Tapered Element Oscillating Microbalance (TEOM, Rupprecht and Patashnick, Model 1400a). TEOM incorporates an inertial balance that directly measures the mass of aerosol accumulated on an exchangeable filter cartridge by monitoring the corresponding frequency changes of a tapered element (Allen et al., 1997).

Besides the on-line measurements, the generated particles were also investigated by transmission electron microscope (TEM) analysis. For this purpose a portion of the ablated particles was collected on a CF200-Cu (Electron Microscopy Science) grid.

3 Results

All the presented results correspond to measurements made when using nitrogen as a carrier gas with a volumetric flow rate of 500 $\mathrm{cm^3\,min^{-1}}$, unless otherwise stated. Aerosol mass concentration measured by the TEOM instrument as a function of the laser fluence can be seen in Fig. 2.The number size distribution of the generated

Title Page
Abstract Introduction
Conclusions References
Tables Figures
◀| |▶
◀ ▶
Back Close
Full Screen / Esc
Printer-friendly Version
Interactive Discussion

carbonaceous particles measured at three different fluences is shown in Fig. 3. There are two identified characteristic modes in the number size distribution with a count median diameter (CMD) in the range of 15 and 100 nm, which are called as primary particles and fractal aggregates in the following, respectively (see below). The segregated number concentrations in these two modes are shown as a function of laser fluence in Fig. 4. The CMD and the full width at half maximum (FWHM) of the fractal aggregate mode at different laser fluences are given in Table 1. The number size distribution of the laser generated carbonaceous particles measured at three different volumetric flow rates of the nitrogen carrier gas using $2\,\mathrm{J\,cm^{-2}}$ fluence can be seen in Fig. 5. Figure 6 shows the measured number size distribution in case of different purging gases at $2\,\mathrm{J\,cm^{-2}}$ laser fluence and $500\,\mathrm{cm^3\,min^{-1}}$ volumetric flow rate. The TEM pictures taken of various generated particles are shown in Fig. 7.

4 Discussion

According to a simplified model, the particle formation process can be divided into three subsequent phases (Gelencsér, 2004):

In the *nucleation phase* etching of the sample induces an ablation plume that contains different vapours and fragments originating from the destroyed target material. Then these components connect with different types of bonds, and the resulting nanoparticles serve as nucleuses in the subsequent phases of particle generation.

In the *coagulation phase* primary particles collide, and due to the favourable energy conditions they form new, spherically shaped particles with a volume roughly equal to the sum of the volumes of the individual particles. However, the surface of the new particles are much smaller than the sum of the surfaces of the colliding ones.

In the *aggregation phase* colliding particles become weakly bonded to one another creating fractal aggregates with a complex morphology.

Nucleation can be classified as a gas to aerosol transition chemical process, while particle evolutions via coagulation or aggregation are physical processes. Coagulation and aggregation are competing processes, the ratio of coalescence and collision time determines their relative dominance (Hawa and Zachariac, 2005):

$$\tau_{\text{coalescence}} > \tau_{\text{collision}} \rightarrow \text{coagulation} \rightarrow \text{spherical particles}$$

$$\tau_{\text{coalescence}} < \tau_{\text{collision}} \rightarrow \text{aggregation} \rightarrow \text{fractal aggregates}$$

As far as our measurement results are concerned (Fig. 2), at fluences below $\sim 0.9\,\mathrm{J\,cm^{-2}}$ the mass concentration of the generated aerosol particles was found to be almost completely independent of the applied fluence, while above this limit the mass concentration increased roughly linearly with the fluence. This can be explained by the fact that at low fluences the excitation causes fragmentations on the irradiated surface, which is a surface phenomenon and thus largely independent from the variation in fluence, while at higher fluences the yield of aerosol generation is proportional to the whole ablation volume determined by the penetration depth of the laser pulse. The latter is a volume effect, wherefore aerosol yield in this regime is scaled by the laser fluence.

Depending on the applied laser fluence three characteristic domains can be identified in the measurement results:

At low fluences the generated carbon aerosol plume dominantly contains a high number of small primary particles (see the curve corresponding to a fluence of $0.7\,\mathrm{J\,cm^{-2}}$ in Fig. 3) supposedly with a spherical shape (such as those shown in the TEM picture in Fig. 7a) and various sizes, while the number of aggregates is low, and they are typically built from a small number of monomers. In this region either the number of primary particles is insufficient for efficient fractal aggregate generation or the primary particles are too small for the aggregation process to take place. In either case the results indicate that in this domain the coalescence time is much shorter than the collision time.

At intermediate fluences there are both primary particles and an increasing number of fractal aggregates in the plume (see the curve corresponding to a fluence of $0.9\,\mathrm{J\,cm^{-2}}$ in Fig. 3). With increasing fluence fractal aggregates with complex morphology (such as those shown in the TEM pictures in Fig. 7b and c) become dominant in the generated aerosol plume (Fig. 4). In this domain, the generated fractal aggregates are characterised with log-normal size distribution with slightly fluence-dependent CMD and FWHM values (Table 1). As it can be seen in Fig. 4, there is still a relatively large number of primary particles in the generated plume. The coalescence time and the collision time are assumed to be roughly equal in this domain.

Finally, above ~ 1.8 J cm^{-2} fractal aggregates become dominant (see the curve corresponding to the fluence of 2.5 J cm^{-2} in Fig. 3), and the yield of primary particles does not increase any further with fluence (Fig. 4). The most probable reason for such behaviour is that at such high fluences all the primary particles in access of a certain limit are consumed by cluster formation. So the primary particles are sources of fractal aggregates, meanwhile the fractal aggregates are gulp of the primary particles. In this region the coalescence time has to be much longer than the collision time.

As it can be seen from the presented results the laser ablation method which we propose here as a tool for particle generation offers various advantages:

- The size of the generated particles ranges from 10 nm to 1100 nm.
- The number concentration of the generated particles can be as high as 10^{7} particle cm^{-3} (in case of 2 J cm^{-2} fluence and nitrogen purging gas with a volumetric flow rate of 200 sccm).
- Depending on the experimental conditions, either small or large particles can be generated with high efficiency. For example, 20 or 600 nm particles can be generated with an efficiency of about 10^{5} particles cm^{-3} by using 2 J cm^{-2} fluence, synthetic air as purging gas with 500 sccm volumetric flow rate and 2 J cm^{-2} fluence, nitrogen as purging gas with 200 sccm volumetric flow rate, respectively.
- Particles with various complexity can be generated (Fig. 7).
- As it can be seen in Fig. 4 the ratio of the number concentrations of aerosol particles in the fractal aggregate mode to the primary particle mode can be varied from 0 to about 5 quasi-linearly by increasing the laser fluence.

- By changing either the laser fluence or the volumetric flow rate of the purging gas it is possible to change the morphology of the generated aerosol in a controlled manner. As it can be seen in Fig. 5, both the segregated number concentration and the CMD value can be increased by reducing the gas flow rate. The number concentration increases because at a lower volumetric flow rate a given volume of the carrier gas resides in the ablation chamber longer, while the emission rate of the ablated particles remains constant. Furthermore, a reduced flow rate increases the probability of particle collision, which results in an increase in the size of the aggregates, i.e. this is why the CMD value increases.

- Finally, as far as the use of different purging gases is concerned, the proposed carbonaceous aerosol generation method offers great flexibility, too. We have demonstrated that by using different mixtures of N_2 and synthetic air as purging gas the particle generation process can be altered drastically and in a well-controlled manner (Fig. 6). Moreover, compared to nitrogen buffer gas the generation of fractal aggregates is largely suppressed in gas mixtures which also contain synthetic air, presumably due to the concomitant oxidation. Further studies are needed to investigate the possibilities and advantages of using other types of purging gases.

As a result of the advantages listed above, the laser ablation method has a high flexibility and consequently it offers the possibility of generating aerosol particles with parameters covering all the atmospherically relevant ranges as far as mass concentration, aerosol modes, size distribution or morphology are concerned.

5 Summary

In this work we generated carbonaceous particles by laser ablation of a high purity graphite disc. The complete microphysical parameters of the generated particles including number concentration, size distribution and morphology were characterised as a function of the generation parameters such as laser fluence, composition and the volumetric flow rate of the purging gas in the reaction chamber. This characterisation proved a unique advantage of the proposed method, i.e. that the micro-physical features of the generated particles can be controlled accurately and independently from one another. The proposed generator can produce particles either with spherical (primary particles) or with complex morphology (cluster aggregates), as well as a controlled mixture of these modes (Figs. 3 and 4) in an extremely wide size range covering the entire climate and health relevant domain. The measured micro-physical properties confirm that the generated particles have properties which are very close to those of atmospheric black carbon. A special advantage of the proposed method is its flexibility in the use of various gases and gas mixtures as local gas ambient during the formation of carbon particle. This opens up the possibility of quantitative investigation of the gas ambient effect on the particle formations (Fig. 6). As a target material not only graphite but e.g. coal samples can be used, as it was already demonstrated before (Ajtai et al., 2010). This gives further flexibility for the generation method.

Acknowledgements. Financial support by the Hungarian Scientific Research Foundation (OTKA, project no. K101905) is gratefully acknowledged. The European Union and the European Social Fund have provided financial support to the project under the project no. TÁMOP-4.2.2.A-11/1/KONV-2012-0047 and TÁMOP 4.2.2.A-11/1/KONV-2012-0060.

References

Ajtai, T., Filep, Á., Kecskeméti, G., Hopp, B., Bozóki, Z., and Szabó, G.: Wavelength dependent mass-specific optical absorption coefficients of laser generated coal aerosols determined from multi-wavelength photoacoustic measurements, Appl. Phys. A-Mater., 103, 1165–1172, 2011.

Allen, G., Sioutas, C., Koutrakis, P., Reiss, R., Lurmann, F. W., and Roberts, P. T.: Evaluation of the TEOM method for measurement of ambient particle mass in urban areas, J. Air Waste Manage., 47, 682–689, 1997.

Bond, T. C., Doherty, S. J., Fahey, D. W., Forster, P. M., Berntsen, T., DeAngelo, B. J., Flanner, M. G., Ghan, S., Kärcher, B., Koch, D., Kinne, S., Kondo, Y., Quinn, P. K., Sarofim, M. C., Schultz, M. G., Schulz, M., Venkataraman, C., Zhang, H., Zhang, S., Bellouin, N., Guttikunda, S. K., Hopke, P. K., Jacobson, M. Z., Kaiser, J. W., Klimont, Z., Lohmann, U., Schwarz, J. P., Shindell, D., Storelvmo, T., Warren, S. G., and Zender, C. S.: Bounding the role of black carbon in the climate system: a scientific assessment, J. Geophys. Res.-Athmos., 118, 1–173, 2013.

Baumgardner, D., Popovicheva, O., Allan, J., Bernardoni, V., Cao, J., Cavalli, F., Cozic, J., Diapouli, E., Eleftheriadis, K., Genberg, P. J., Gonzalez, C., Gysel, M., John, A., Kirchstetter, T. W., Kuhlbusch, T. A. J., Laborde, M., Lack, D., Müller, T., Niessner, R., Petzold, A., Piazzalunga, A., Putaud, J. P., Schwarz, J., Sheridan, P., Subramanian, R., Swietlicki, E., Valli, G., Vecchi, R., and Viana, M.: Soot reference materials for instrument calibration and intercomparisons: a workshop summary with recommendations, Atmos. Meas. Tech., 5, 1869–1887, doi:10.5194/amt-5-1869-2012, 2012.

Chakrabarty, R. K., Moosmüller, H., Arnott, W. P., Garro, M. A., Slowik, J. G., Cross, E. S., Han, J.-H., Davidovits, P., Onasch, T. B., and Worsnop, D. R.: Light scattering and absorption by fractal-like carbonaceous chain aggregates: Comparison of theories and experiment, Appl. Optics, 46, 6990–7006, 2007.

Gelencsér A.: Carbonaceous Aerosol, Springer-Verlag GmbH, 2004.

Hand, J. L., Malm, W. C., Laskin, A., Day, D., Lee, T., Wang, C., Carrico, C., Carrillo, J., Cowin, J. P., Collett, J., and Iedema, M. J.: Optical, physical, and chemical properties of tar balls observed during the Yosemite Aerosol Characterization Study, J. Geophys. Res., 110, D21210, doi:10.1029/2004JD005728, 2005.

Hawa, T. and Zachariac, M.: Coalescence kinetics of unequal sized nanoparticles, J. Aerosol Sci., 37, 1–15, 2006.

Hopp, B., Kecskeméti, G., Smausz, T., Ajtai, T., Filep, A., Utry, N., Kohut, A., Bozóki, Z., and Szabó, G.: Characterization of excimer laser ablation generated pepsin particles using multiwavelength photoacoustic instrument, Appl. Phys. A-Mater., 107, 429–435, 2012.

IPCC: Summary for Policymakers, in: Climate Change 2007: The Physical Science Basis. Contribution of Working Group I to the Fourth Assessment Report of the Intergovernmental Panel on Climate Change, edited by: Solomon, S., Qin, D., Manning, M., Chen, Z., Marquis, M., Averyt, K. B., Tignor, M., and Miller, H. L., Cambridge University Press, Cambridge, United Kingdom and New York, NY, USA, available at: http://www.ipcc.ch/pdf/assessment-report/ar4/wg1/ar4-wg1-spm.pdf (last access: 9 June 2011), 2007.

Jerret, M., Burnett, R. T., Ma, R. J., Pope, C. A., Krewski, D., Newbold, K. B., Thurston, G., Shi, Y. L., Finkelstein, N., Cale, E. E., and Thun, M. J.: Spatial analysis of air pollution and mortality in Los Angeles, Epidemiology, 16, 727–736, 2005.

Kirchstetter, T. W. and Novakov, T.: Evidence that the spectral dependence of light absorption by aerosols is affected by organic carbon, J. Geophys. Res., 109, D21208, doi:10.1029/2004JD004999, 2004.

Pope, C. A. III and Dockery, D. W.: Epidemiology of particulate effects, Air Poll. Health, 31, 673–705, 1999.

Schnaiter, M., Horvath, M., Möhler, O., Naumann, K. H., Saathol, H., and Schöck, O. W.: UV-VIS-NIR spectral optical properties of soot and soot-containing aerosols, Aerosol Sci., 34, 1421–1444, 2003.

Schnaiter, M., Gimmler, M., Llamas, I., Linke, C., Jäger, C., and Mutschke, H.: Strong spectral dependence of light absorption by organic carbon particles formed by propane combustion, Atmos. Chem. Phys., 6, 2981–2990, doi:10.5194/acp-6-2981-2006, 2006.

Seinfeld, J. H. and Pandis, S. N.: Atmospheric Chemistry and Physics: From Air Pollution to Climate Change, Wiley-Interscience, New York, NY, ISBN9780471178163, 1998.

Solomon, S., Qin, D., Manning, M., Alley, R. B., Berntsen, T., Bindoff, N. L., Chen, Z., Chidthaisong, A., Gregory, J. M., Hegerl, G. C., Heimann, M., Hewitson, B., Hoskins, B. J., Joos, F., Jouzel, J., Kattsov, V., Lohmann, U., Matsuno, T., Molina, M., Nicholls, N., Raga, G., Overpeck, J., Ramaswamy, V., Ren, J., Rusticucci, M., Somerville, R., Stocker, T. F., Whetton, P., Wood, R. A., and Wratt, D.: Technical summary, in: Climate Change 2007: The Physical Science Basis. Contribution of Working Group I to the Fourth Assessment Report of the Intergovernmental Panel on Climate Change, edited by: Solomon, S., Qin, D., Manning, M., Chen, Z., Marquis, M., Averyt, K. B., Tignor, M., and Miller, H. L., Cambridge University Press, Cambridge, UK and New York, NY, USA, 2007.

Table 1. Various parameters of the fractal aggregate mode as a function of the laser fluence in case of nitrogen carrier gas with a volumetric flow rate of 500 cm^3 min^{-1}.

Fluence [J cm^{-2}]	1.25	1.5	1.7	1.9	2.1	2.3	2.5	2.8
CMD [nm]	175.4	152.9	147.2	147.4	137.9	157.6	158	162.8
FWHM [nm]	233.8	196.9	158.3	157.4	137.1	163.8	164.7	169.3
Modal number concentration [10^6 cm^{-3}]	0.8	1	1.8	2.3	2.8	3.3	3.6	4.3

AMTD
7, 10159–10178, 2014
Characterisation of laser generated carbonaceous particles
T. Ajtai et al.

Title Page
Abstract Introduction
Conclusions References
Tables Figures
◀ ▶
Back Close
Full Screen / Esc
Printer-friendly Version
Interactive Discussion

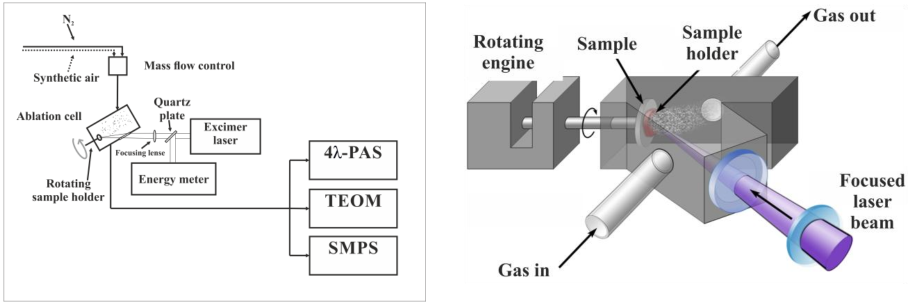

Figure 1. The schematic scheme of the experimental setup (left) and the modified PLD chamber (right).

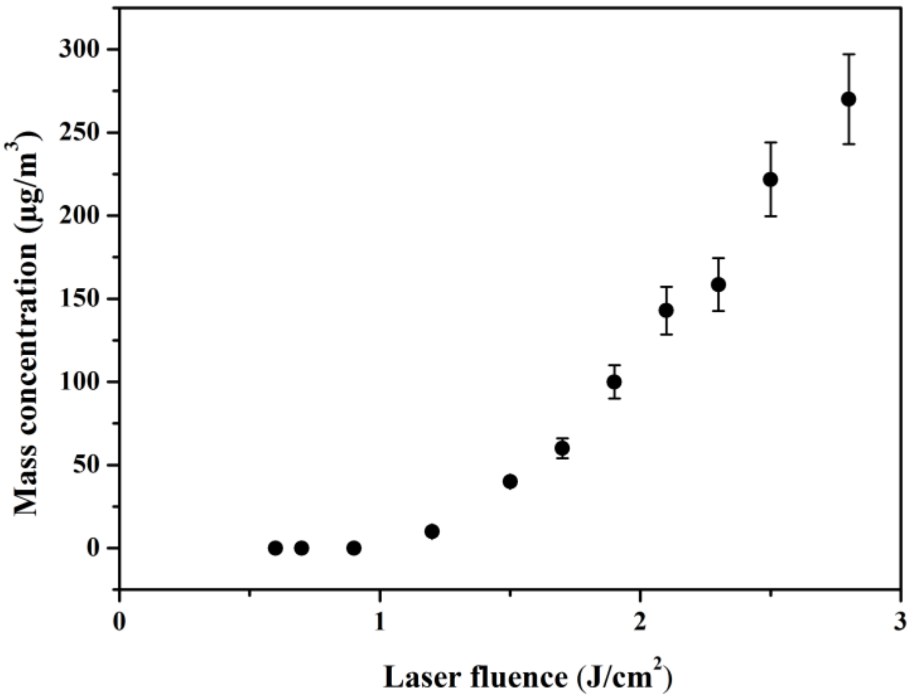

Figure 2. Mass concentration of ablation generated carbonaceous aerosol particles as a function of the fluence of the KrF excimer laser.

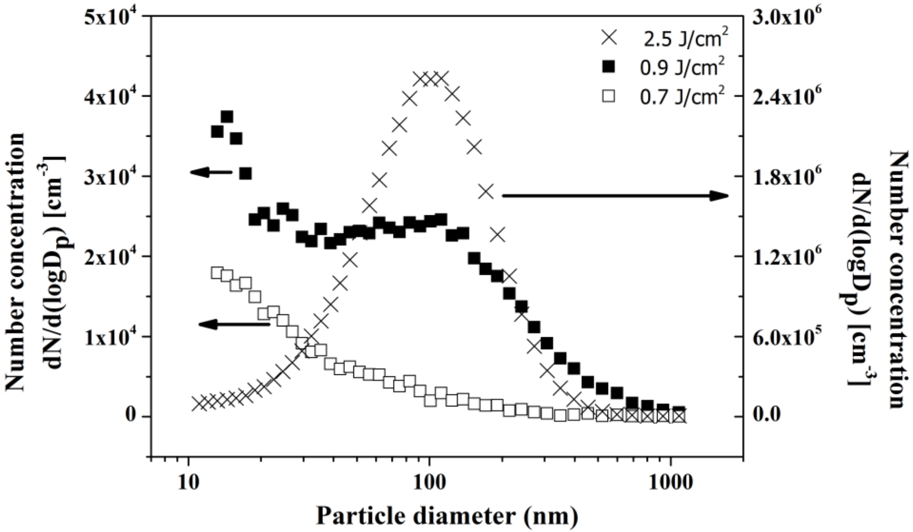

Figure 3. Number size distribution of the generated carbonaceous particles at three different laser fluences. Note: the right y axis applies for the $2.5\,\mathrm{J\,cm^{-2}}$ fluence.

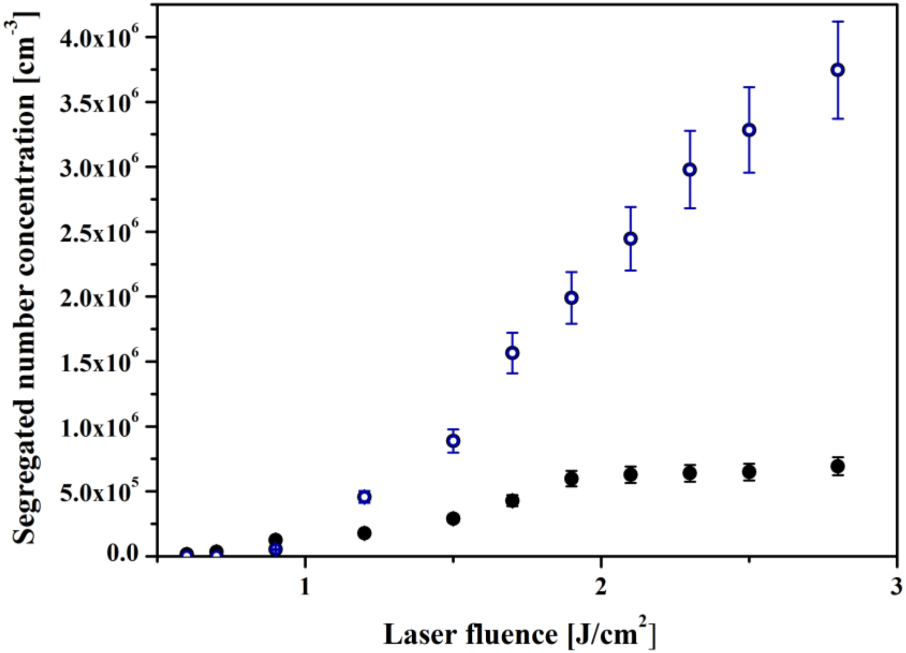

Figure 4. Segregated number concentrations in the two characteristic modes as a function of the laser fluence. Closed circles: primary particles, open circles: fractal aggregates.

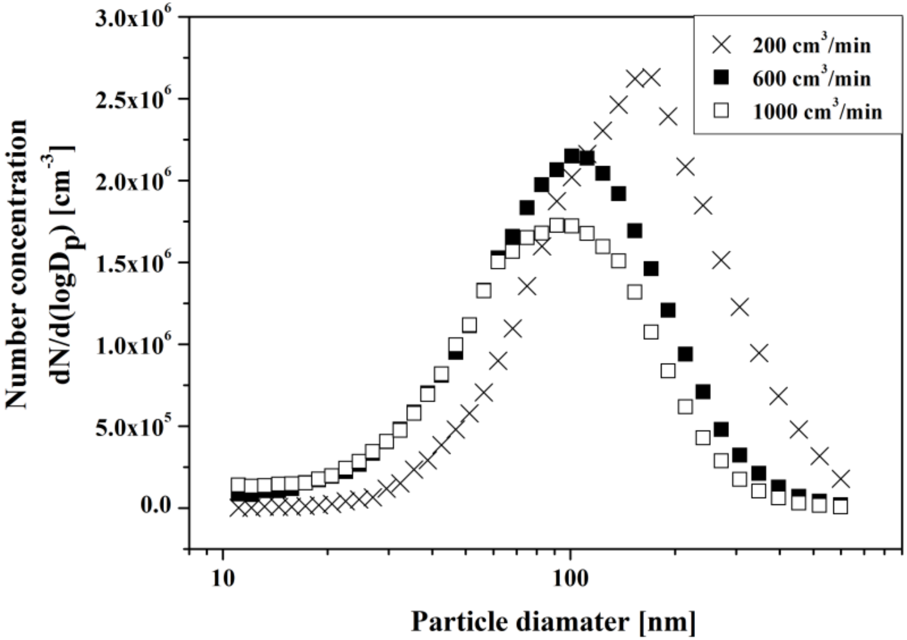

Figure 5. Number size distribution of the generated carbonaceous particles at three different volumetric flow rates of nitrogen purging gas at 2 J cm^{-2} fluence.

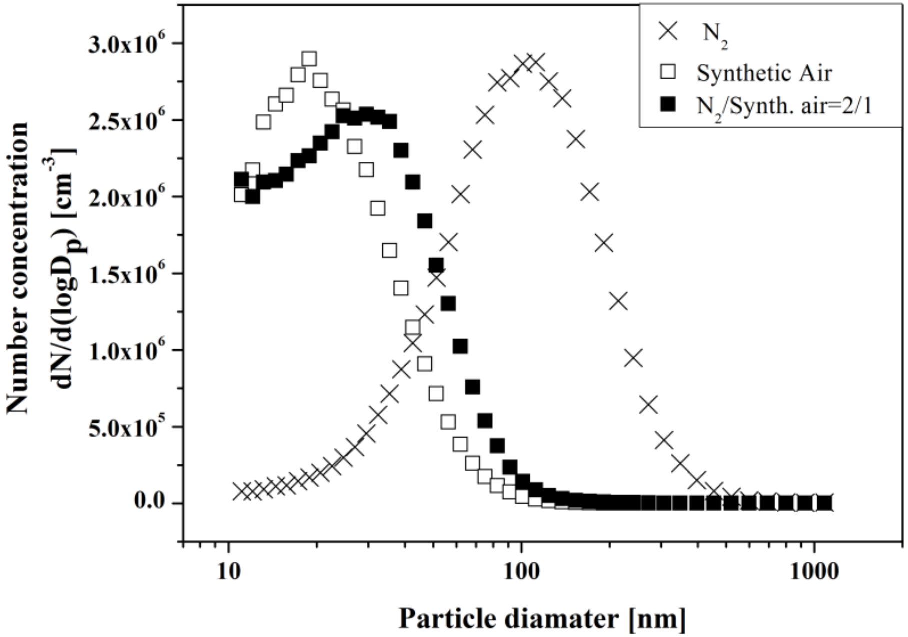

Figure 6. Number size distribution of the laser ablation generated carbonaceous particles by applying different carrier gases with a volumetric flow rate of 500 cm^3 min^{-1} at 2 J cm^{-2} fluence.

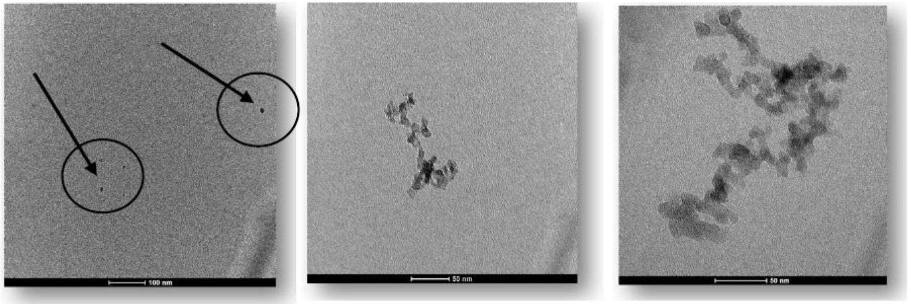

Figure 7. TEM images of various laser generated carbonaceous aerosol particles.